
CFD MODEL DEVELOPMENT FOR A FINAL EFFECT EVAPORATOR

By

S.N. PENNISI^{1,2}, J.-L. LIOW² and P.A. SCHNEIDER²

¹ *Sugar Research Institute, Nebo Road, Mackay, Queensland 4740*

² *School of Engineering, James Cook University, Townsville, Queensland 4811*

s.pennisi@sri.org.au, jongleng.liow@jcu.edu.au, phil.schneider@jcu.edu.au

KEYWORDS: Numerical, Evaporator, CFD

Abstract

THE use of computational fluid dynamics (CFD) modelling tools in the engineering design process has become increasingly popular in recent times as a result of beneficial outcomes from several studies. Sugar mill Roberts evaporators are likely to have non-ideal juice flow characteristics and design improvements could be realised if a suitable computational model were developed. The model would be a useful tool for predicting broad trends in fluid flow behaviour when process equipment modifications are implemented. In this paper, a numerical model is presented for the single-phase fluid flow inside an evaporator vessel. The model is a one-quarter wedge of the entire vessel utilising two planes of symmetry to reduce the size of the mesh required. The model incorporates the effect of temperature and brix on the fluid properties. A heat source is used to model the heat flows through the calandria and momentum sources are used to model the effect of the vertical heating tubes in the calandria section and also the buoyancy forces generated by the production of vapour. A series of experiments was conducted to gather brix and temperature measurements at certain points within the juice space below the calandria. These data were compared with the predictions and used to judge the model's ability to predict fluid flow. The predictions show good agreement with factory data. Both the measured and predicted brix and temperature distributions are well mixed, with the majority of juice in the region below the calandria at conditions close to those reporting to the outlet. The model presented cannot predict the heat transfer performance of the calandria section and it has not been run outside the conditions normally encountered in a typical vessel. Both of these issues have been identified as direction for future development. The model has demonstrated its ability to accurately predict the fluid flows inside the entire vessel within these constraints.

Introduction

The use of computational fluid dynamics (CFD) models as an engineering design tool has become increasingly popular in recent times. Sugar mill Roberts evaporators are likely to have less than perfect flow characteristics and the heat transfer performance of these vessels could be improved if these flow characteristics could be improved. CFD modelling is a useful tool in this process, if a suitable computational model can be developed. Existing CFD models have limited application since they do not include the heat and mass transfer mechanisms occurring inside the

calandria. Although there have been a number of papers dealing with heat transfer efficiency in evaporators (Watson, 1986, 1987), there is a dearth of work on the direct numerical simulation. Rouillard (1985) carried out experimental studies of the convective boiling of sugar solutions and developed a one-dimensional model to predict mass flow and evaporation rates inside the heating tubes of vacuum pans. Stephens and Harris (1999) modelled flow within a single tube in the calandria of a vacuum pan, using uni- and axisymmetric Eulerian two-phase flow models. Steindl and Ingram (1999) presented CFD modelling results for a Roberts evaporator. Their model was limited to the juice flow in the region below the calandria with a mass sink for water evaporation as a boundary condition accounting for the boiling in the calandria.

Stephens (2001) modelled a vacuum pan and demonstrated that modelling the flow in the calandria alone is extremely complex, due to the boiling phenomena. His approach was to model the fluid regions above and below the calandria comprehensively and interface these regions with a simplified mathematical model of the fluid flow inside the calandria, thus providing useful engineering solutions. Combining the simplified approach of Steindl and Ingram (1999) and the segmented approach of Stephens (2001) has enabled the development of our numerical model of an evaporator effect. Figure 1 shows the three fluid regions used to represent the evaporator for this study; those regions being above the calandria, the calandria itself and below the calandria.

In the absence of data describing the fluid flow in the heating tubes of the calandria, a model has been developed where the calandria has been simplified with a mass and heat balance model, which is linked to the CFD model of the region below the calandria. This represents an important first step in modelling the evaporator. The model's ability to predict fluid flow is determined by comparing temperature and brix predictions with measurements taken from a factory vessel.

In the absence of any pre-existing data suitable for comparison with CFD models, a series of experiments was designed and carried out on a final effect vessel. These data will be presented later in this paper.

The study vessel for modelling and experiments

The physical layout of the study vessel was used for all of the model development. This vessel was chosen because it is a final vessel and therefore experiences the largest variation in fluid properties. The vessel also required minimal modifications to allow experimental comparison data to be gathered from it. The mill has a number of flow rate and other measurements already incorporated into the control system for the evaporator set. This was seen as an advantage when gathering factory data from the vessel.

The vessel diameter is 9.26 m, the calandria consists of 18 553 heating tubes, each 44.45 mm o.d. and 1.981 m in length and an array of 56 down-takes, each of 150 mm nominal bore (NB), distributed uniformly among the heating tubes. The total heating surface area of the vessel is 5265.7 m².

Juice is fed into the vessel via a four-point entry with a single central outlet. At the inlet, an inverted L-shaped deflector plate is placed over the vertical inlet pipe. The horizontal section of the plate completely covers the inlet pipe and the vertical section is on the side facing the centre of the vessel and runs to the floor of the vessel. Thus, at each inlet, the juice flow is diverted outwards. Figures 1 and 2 show the relevant dimensional details of the vessel.

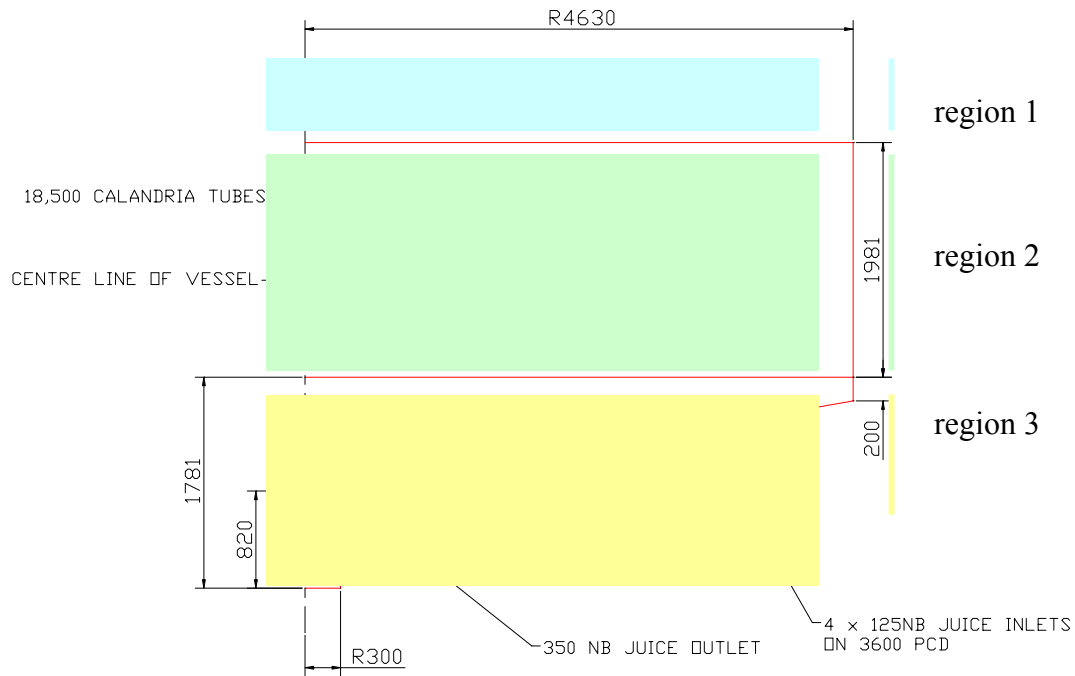


Fig. 1—Side view of the vessel used for this study.

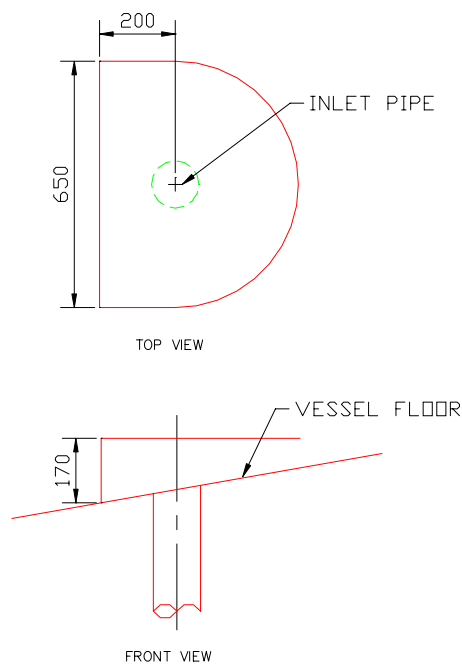


Fig. 2 – Details of the deflector plate over the inlet pipe.

Model description

Physical geometry *(For nomenclature used in this paper, see Appendix B)*

The vessel displays one-quarter symmetry, which was used to reduce the size of the computational mesh required. The regions above and below the calandria were modelled in detail with the conservation equations. The free surface in the region above the calandria was modelled as a rigid boundary with free slip. The calandria itself includes an array of small down-takes. These down-takes have not been included in the model geometry in an attempt to simplify the mesh required to run the simulation. The calandria was modelled as a series of mass, energy and momentum sources, to account for the simplifying assumption.

For simplicity, the effect of the calandria tubes was modelled as a pressure drop resulting from the flow of fluid through the heating tubes, using frictional pipe flow equations. It was assumed that the fluid flow was predominantly in the vertical direction due to the buoyancy generated by boiling within the tubes and the physical presence of the walls of the tubes. To ensure that the vertical flow dominates, the pressure drop in the horizontal direction was set to a value much larger than the maximum pressure drop in the vertical direction. In this work, the pressure drop in the two horizontal directions (x and z) were modelled as momentum sources, according to

$$\frac{dP}{dx} = -100.0|u|^2 \quad (1)$$

$$\frac{dP}{dz} = -100.0|w|^2 \quad (2)$$

The pressure drop in the vertical direction (y) was approximated by

$$\frac{dP}{dy} = -f \left(\frac{|v|^2 \rho_m}{2A_o d} \right) \quad (3)$$

The magnitude of the velocity components is used since the flow is bi-directional in the vertical plane, i.e. up and down the heating tubes. The A_o term accounts for the tube area relative to the calandria section area.

The friction factor (f) is a modified version of the Colebrook equation, see Vennard and Street (1982) for further information on the Colebrook equation. Since the flow in the calandria is predominantly in the laminar or transitional regions, the friction factor equation was modified to avoid mathematical singularities caused by the discontinuity of the friction factor curves in the transitional flow regime. The final form of the function for f is as follows

$$f = 0.027 + \frac{53.33}{\text{Re}} \quad (4)$$

Re in the equation above is the liquid Reynolds number using the internal diameter of the heating tube as the length scale. Figure 3 shows a plot of the standard friction factor equations for turbulent and laminar flow and the modified equation applied in this case.

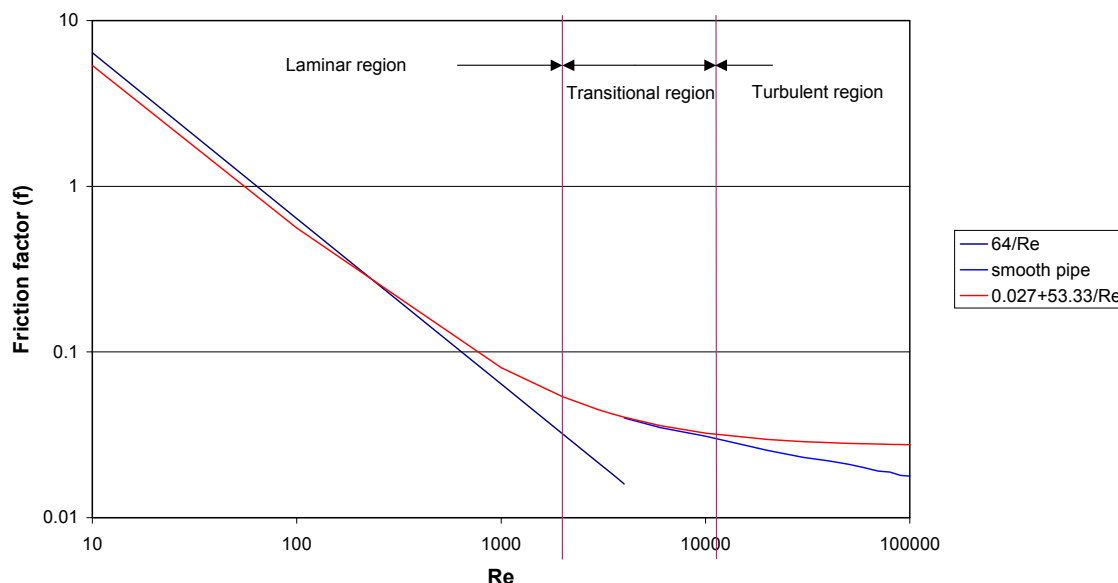


Fig. 3—Plot of friction factor versus Reynolds number.

Figure 3 shows that the modified equation slightly under-estimates the friction factor at very low Reynolds numbers and slightly over-estimates the friction factor at higher Reynolds numbers in the laminar region. The modified equation also over-estimates the friction factor in the turbulent region but allows a smooth transition through the transitional region. This is the major benefit of this approximation over the standard equations. The overestimation of friction factor in the turbulent region is the largest source of error. However, this is not important since the largest Reynolds number predicted for flow in the evaporator tubes is approximately 7000. According to Figure 3, such flow is still within the transitional region.

The momentum sources detailed in equations 1 and 2 above proved inadequate in restricting the fluid flow to the vertical direction. This was because the magnitude of the momentum source could not be increased above this value without causing numerical errors. These numerical errors arise from the magnitude of the momentum source in the horizontal plane being significantly larger than the magnitude in the vertical direction. To assist in straightening the flow, 56 internal frictionless walls were placed inside the calandria. The resultant fluid flow in the calandria section was a very close approximation to a one-dimensional flow, with fluid moving up and down the calandria heating tubes only. The final model showed that the average fluid velocity in the horizontal plane was less than 10% of the vertical

Heat flows

The model does not predict the heat transferred through the calandria to the fluid. Instead the total heat flow through the calandria is applied as a boundary condition. This is a limitation in the model's ability to predict vessel performance, but is necessary for the development and comparison work undertaken as part of this study.

The total thermal energy, Q_{tot} , released by the condensing steam, neglecting thermal losses through the walls of the vessel, was assumed to pass to the juice as latent heat of evaporation,

producing vapour and sensible heating of the remaining liquid, due to the effect of boiling point elevation.

$$Q_{tot} = \dot{m}_e h_{fg} + \dot{m}_{in} C_p T_{bpe} \quad (5)$$

In equation 5, T_{bpe} is evaluated at the outlet and C_p is evaluated at the inlet. This is due to a limitation within the software that does not allow the specific heat capacity to be calculated as a function of brix and temperature. Instead, the specific heat capacity for the entire fluid flow was set to a constant value evaluated at the inlet juice conditions.

Neglecting heat losses to atmosphere, the total quantity of heat flowing through the calandria was assumed to be converted into the latent heat of evaporation and would leave with the liquid phase with the vapour, the remainder would flow into the liquid as sensible heating. The latent heating and the sensible heating portions of the total heat flow were modelled as two different sources in the calandria section, with an overall heat balance being performed to ensure the total quantity of heat flowing through the calandria is correct. This assumption is valid provided the evaporation rate, described in the next paragraph, is predicted correctly.

Evaporation

The conversion of the water in the juice to vapour was modelled by linking a mass sink term to the temperature of the fluid as follows

$$\dot{m}_{evap} = \begin{cases} 0, T < T_{sat} + T_{bpe} \\ \dot{m}_e, T \geq T_{sat} + T_{bpe} \end{cases} \quad (6)$$

The average evaporation is switched on or off if the fluid temperature is at, or below, the saturation temperature plus the boiling point elevation temperature.

Fluid quality

The production of vapour in the calandria section, although not modelled specifically, was accounted for by calculating the quality of the multi-phase fluid that would otherwise have been produced. Fluid quality in the calandria section was calculated according to the following expression based on the velocity of the gaseous and liquid phases

$$X = \frac{\rho_g v_g}{\rho_l v_l + \rho_g v_g} \quad (7)$$

The calculation of fluid quality via equation 7 assumes that the cross-sectional area occupied by the liquid phase is equal to that occupied by the gaseous phase, as it flows past each node. In reality, the presence of the vapour phase would displace a portion of the liquid phase and so the two areas would be different. However, this assumption is necessary in this case to simplify the equations used, thus establishing a workable model.

The vertical velocity component for the liquid phase (v_l), as used in equation 7 above, is predicted at each node as part of the solution and is used accordingly. The vertical velocity component for the gaseous phase (v_g) is calculated based on the predicted evaporation rate (\dot{m}_{evap}) as detailed in equation 6.

Since the quality of the fluid is linked to evaporation, which only occurs in the calandria section, the fluid quality elsewhere in the vessel is zero, i.e. no gaseous phase is present. In reality, this is not the case because, in all vessels, apart from the first effect, the juice enters with a small amount of superheat that flashes vapour upon entry. This vapour cannot be modelled using the method described above and a more complicated method is required. In order to simplify the model, the amount of vapour that flows into the vessel at inlet was assumed to evaporate in the calandria section. This was necessary to ensure that the overall mass balance remained accurate since in this case the quantity of vapour produced by flashing at the inlet is approximately 15 t/h as compared to a total evaporation rate of approximately 110–115 t/h. It was believed that the additional 10% of the total evaporation rate could not simply be ignored.

Buoyancy forces

The buoyancy forces generated by the production of vapour in the calandria section were modelled as a momentum source according to the following

$$\frac{dP}{dy} = -g(\rho_m - \rho_{ref}) \quad (8)$$

In equation 8 $\rho_{ref} = 1000 \text{ kg}\cdot\text{m}^{-3}$ and ρ_m is calculated according to the following

$$\frac{1}{\rho_m} = \frac{X}{\rho_g} + \frac{(1-X)}{\rho_l} \quad (9)$$

where X is the juice quality. The buoyancy forces calculated by equation 8 were applied as a momentum source term to the entire fluid domain. In the calandria section, this momentum source was simply added to the frictional pipe flow pressure drop calculated by equation 3.

Brix (sugar concentration)

The brix (B) was modelled as an additional variable in the transport equation and was allowed to be diffusive. The diffusivity coefficient was set to the average kinematic viscosity of the fluid at inlet and outlet conditions. The average viscosity was chosen since it provides a good means of approximation over the range of fluid conditions experienced inside the entire vessel. However, the magnitude of the diffusivity coefficient has little impact on the results since the convective transport dominates the diffusion of B .

Fluid properties

The fluid properties are functions of the fluid temperature (T) and the brix (B) and correlated through equations 10 to 13, as listed in Appendix A.

Turbulence modelling

Turbulence generated within any fluid flow is not modelled directly due to the large computing power required to solve the Navier-Stokes equations. Instead, a means of approximating the turbulence quantities is used. Fletcher (1991) provides further details on turbulence modelling. There are a number of standard turbulence models that have been developed and the discussion of details of such models is outside the scope of this paper.

The standard $k-\varepsilon$ turbulence model was used for this investigation. Although some areas within the fluid flow are reasonably slow moving, and therefore possibly laminar, the turbulence model produced caused no problems with the stability of the simulations.

Solution of the model

All of the equations detailed above were solved using the CFD package, CFX¹ v5.5.1. The simulations were computed on a Pentium IV 2.4 GHz processor with 2 Gb of RAM, running Linux v7.3.

Factory measurements

In order to provide validation of the model, plant measurements were made to provide comparative data. These measurements included brix and temperature at a number of locations in the juice space below the calandria. Measurements required to provide boundary conditions were also taken. Measurements were taken at the inlet, outlet and at three locations mid-way through the flow path from inlet to outlet. Figure 4 shows further details of the measuring point locations. The three sample points were located radially in a line from one of the inlets towards the central outlet. Point A is $2/3$ of the vessel radius away from the centre-line, Point B is $1/3$ of the vessel radius away from the centre-line and Point C is on the centre-line of the vessel.

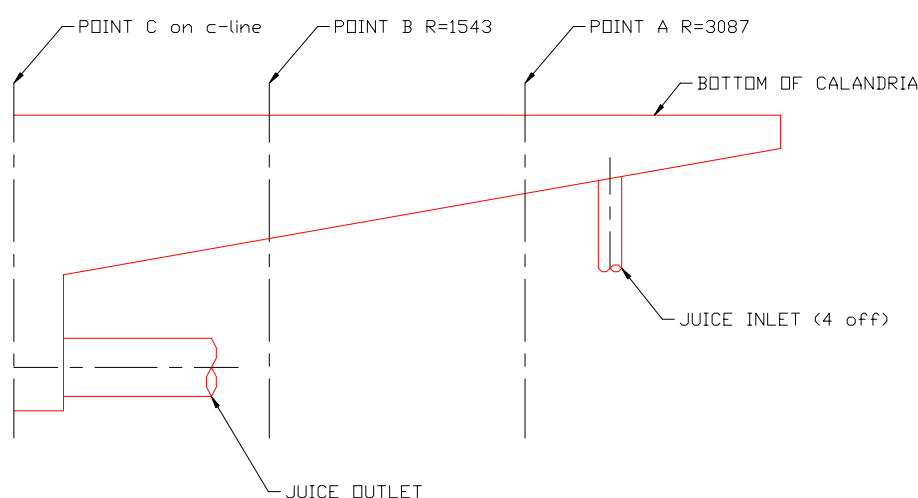


Fig. 4—Location of the sample points on the actual vessel.

¹ CFX software distributed in Australia by Australian Trade Development (ATD) International Ltd, Melbourne, Australia.

Sampling tubes were inserted vertically through the bottom of the vessel for a range of distances below the bottom of the calandria. Table 1 shows the distances below the calandria for the four data sets used for this comparison. Positive values in Table 1 denote distances above the bottom tube-plate (i.e. inside the heating tubes) and negative values denote distances below the bottom tube-plate.

Table 1 – Sample point locations.

Point Test No:	Vertical distance (m)			
	1	2	3	4
A	0.0	0.0	-0.2	-0.2
B	0.136	-0.064	-0.064	-0.264
C	-0.408	-0.608	-0.608	-0.808

Due to natural fluctuations within the system, data points were logged for a 30-minute period to provide an average value. This period of logging also provided information on the extent of variation with time and the long-term performance of the vessel. In general, the brix data varied between ± 4 –5% of the total brix change from inlet to outlet and the temperature data varied between $\pm 0.5^\circ\text{C}$.

Further details of the tests conducted are given in Pennisi (2002). Those data relevant to this study have been included in tabular form in the relevant section.

Comparing model predictions with factory data

Four tests were conducted on the vessel. Table 2 shows a summary of the processing conditions measured at the time.

Table 2—Summary of the processing conditions experienced for the 4 tests.

Variable	Test No. 1	Test No. 2	Test No. 3	Test No. 4
Juice brix at inlet (%)	35.6	36.3	37.7	38.1
Calandria pressure (kPa abs)	62.3	64.1	47.9	47.4
Headspace pressure (kPa abs)	13.7	13.8	14.6	14.8
Condensate flow rate (t/hr)	131.9	131.2	137.6	134.3

Table 2 shows a significant variation in the processing conditions between tests no. 1 and 2 and tests no. 3 and 4. This is due to the first two tests being conducted one day prior to cleaning and the last two tests being conducted immediately after a clean. This was done deliberately so as to gain data from the maximum range of processing conditions experienced by the vessel.

Table 3 shows the results of all comparisons. The measured and predicted values are in good agreement, averaging a difference of only -3.4% for brix and $+1.3\%$ for temperature. This demonstrates that the model is able to predict the brix and temperature fields to within acceptable limits of accuracy, in spite of the simplifying assumptions made.

Table 3 – Comparison of measured data against model predictions.

	Temperature (°C)		brix (% wt)	
	Measured	Predicted	Measured	Predicted
Test No. 1				
A	55.1	55.7	63.5	60.4
B	55.0	55.9	65.0	62.2
C	57.0	55.9	63.6	62.3
outlet	55.2	55.9	63.1	62.2
Test No. 2				
A	55.5	55.9	64.4	61.9
B	55.1	55.9	65.7	62.2
C	57.3	55.9	64.5	62.6
outlet	55.4	55.9	63.7	62.5
Test No. 3				
A	55.5	58.0	68.5	66.3
B	55.1	58.1	72.9	66.6
C	57.3	58.1	67.1	66.5
outlet	55.4	58.1	67.5	66.5
Test No. 4				
A	58.0	58.0	68.1	64.4
B	57.3	58.1	69.1	65.6
C	58.8	58.1	66.7	65.8
outlet	57.4	58.1	67.1	65.8

Table 2 shows that the measured brix at point B is always higher than the other three comparison points, albeit by only a couple of percentage units. Since this is a consistent trend in the measured data, it must be recognised that the same difference between point B and the others is not being reproduced by the predictions to the same degree. This demonstrates that while the model is capable of predicting the broad trend of high brix material in a majority of the juice space below the calandria, it is not capable of predicting the localised high brix material seen at point B.

The predictions show that the region around the inlet has large velocity gradients and it is clear from the predictions that the design of the inlet system has a major influence on the fluid flow in the remainder of the vessel. Pennisi *et al.* (2003) discusses the effect of the inlet design further. The results presented in that paper formed the preliminary work for the results displayed here.

Discussion

The CFD model presented here has demonstrated its ability to predict the brix and temperature field within the vessel chosen for this study. Although only one vessel has been used for the study so far, it is a final vessel in a set and therefore experiences the largest variation in fluid properties. Confidence in the model comes from knowing that if it can produce accurate predictions on a final vessel. It is expected that the model should be capable of producing accurate predictions on an earlier vessel where the process conditions are less variable. Further investigations are required to take the model and apply it to an earlier vessel to demonstrate its ability to perform over a wide range of conditions.

A number of simplifying assumptions have been made in order to develop the model to its current stage where it can make reliable predictions. The results gathered so far show that the simplification have not detracted from the model's ability to predict large trends in the wider fluid flow, but the model is limited in its ability to predict smaller, more localised differences. Even so, the predictions are still useful when applied as an engineering design tool. The most significant assumption associated with the work presented here is neglecting gaseous (vapour) phase from the simulation, but accounting for its effect on the liquid phase through mathematical relationships. This assumption provides a major advantage to the modelling exercise since modelling of the multi-phase process would be significantly more difficult.

The current model requires the quantity of heat flowing through the calandria to be specified as a boundary condition. While this is useful for validation of the model (where the heat transfer performance is known) and for examining small changes to the vessel geometry that are not expected to greatly affect the heat transfer performance of the vessel, the model would ideally predict heat transfer performance. This will then allow its use as a design tool when considering radical changes to vessel geometry that are able to achieve significant improvements in heat transfer performance. This has been identified as a major focus for future development and is currently being investigated.

Even though the sample points chosen were a long distance apart, all of the sampling points were at very similar brix and temperature and comparable to the brix and temperature at the outlet. This is not desirable for comparison purposes since all of the data lies within a narrow band. However, this is a limitation of the data available for this study and any future experiments will aim to improve the spread of the data set.

The factory data gathered as part of this investigation show good agreement with the model predictions, although the data range is quite small. In order to gain more confidence in the model's ability to accurately predict the fluid flows, further experimental data are required from the region around the inlet, since this is where the largest brix, temperature and velocity gradients exist.

Conclusion

Three-dimensional numerical models of the liquid phase fluid flow inside the entire vessel geometry of a sugar mill evaporator have been presented. The model is capable of predicting trends for process conditions similar to those normally experienced in the final vessel of an evaporator set. While not demonstrated here, it is expected that little development work would be required to successfully apply the same modelling technique to an earlier effect vessel, due to the less extreme changes in fluid properties.

The simplifying assumptions made as part of this development work have not detracted from the model's ability to produce useful predictions. While the gaseous (vapour) phase has not been modelled specifically, the allowances made for the presence of vapour are adequate for the intended purposes of this model.

The model presented here has not been tested over the entire range of processing conditions normally experienced in an evaporator station, nor does it have the ability to predict the heat transfer performance of the vessel. Both of these issues have been identified as key future requirements and work is currently underway to address them.

Both the measured and predicted data show that the brix and temperature distribution in the region below the calandria is considered to be less than ideal. This provides opportunities for improvements to the current standard Roberts evaporator design and highlights the need for the development of a suitable CFD modelling tool.

Acknowledgements

The authors acknowledge the funding contributions provided by the Department of State Development of the Queensland Government and the Australian Research Council. The authors also acknowledge the staff of the Sugar Research Institute and Proserpine Mill for their assistance in planning and conducting the factory experiments and Proserpine Mill for allowing access to their evaporator vessel.

REFERENCES

- Fletcher, C.A.J.** (1991). Computational Techniques for Fluid Dynamics, Volume 2, Second Edition. London, England, Springer-Verlag.
- Peacock, S.** (1995). Predicting physical properties of factory juices and syrups. *International Sugar Journal* 1995, Vol. 97, No. 1162. John Roberts & Sons, Manchester, England.
- Pennisi, S.N.** (2002). Summary of evaporator test results—Proserpine Mill, #4 evaporator 2002 crushing season, Sugar Research Institute (SRI) internal report 11/02. SRI, Mackay, Queensland, Australia.
- Pennisi, S.N., Liow, J.-L., and Schneider, P.A.** (2003). CFD model development for sugar mill evaporators, 3rd International Conference on CFD in the Minerals and Processing Industries, CSIRO, Melbourne, Australia, 9–12 Dec.
- Rouillard, E.E.A.** (1985). A study of boiling parameters under conditions of laminar non-Newtonian flow with particular reference to massecuite boiling, PhD thesis, University of Natal.
- Steindl, R.J.** (1981). Viscosity estimations for pan stage materials. Sugar Research Institute (SRI) technical circular 59. SRI, Mackay, Queensland, Australia.
- Steindl, R.J. and Ingram, G.D.** (1999). Improved evaporator performance through circulation modelling. Sugar Research Institute (SRI) syndicated project report 7/99. SRI, Mackay, Queensland, Australia.
- Stephens, D.W.** (2001). Modelling natural circulation in batch vacuum pans, PhD thesis, James Cook University.
- Stephens, D.W. and Harris, J.** (1999). Modelling convective boiling of molasses, 2nd International Conference on CFD in the Minerals and Processing Industries, CSIRO, Melbourne, Australia, 6–8 Dec, 393–398.
- Vennard, J.K. and Street, R.I.** (1982). Elementary Fluid Mechanics, Sixth Edition. Brisbane, Australia, John Wiley & Sons.

Watson, L.J. (1986). Heat transfer performance in evaporators Part 1. Theory and Mechanisms. Sugar Research Institute (SRI) technical report 191. SRI, Mackay, Queensland, Australia.

Watson, L.J. (1987). Heat transfer mechanisms in evaporators. Proc. Aust. Soc. Sugar Cane Technol., 9: 221–227.

APPENDIX A – CORRELATIONS USED

Density, Watson (1986):

$$\rho_l = 1005.3 - 0.22556T - 2.4304 \times 10^{-3} T^2 + 3.7329B + 0.01781937B^2 \quad (10)$$

Viscosity, Steindl (1981):

$$\mu_l = 4.3 \times 10^{-4} \exp[3.357(B - 0.3155(T - 50))/116.8 - (B - 0.3155(T - 50))] \quad (11)$$

Thermal conductivity, Watson (1986):

$$\kappa = 0.574 + 1.699 \times 10^{-3} T - 3.608 \times 10^{-6} T^2 - 3.528 \times 10^{-3} B \quad (12)$$

Boiling point elevation, Peacock (1995):

$$T_{bpe} = 6.064 \times 10^{-5} \left(\frac{(273.15 + T)^2 B^2}{(373.15 - T)^{0.38}} \right) \times (5.84 \times 10^{-7} (B - 40)^2 + 7.2 \times 10^{-4}) \quad (13)$$

APPENDIX B–NOMENCLATURE

A_o	open area ratio of the tube-plate
B	brix (sugar concentration by weight) (%)
C_p	specific heat capacity (J/kg/K)
d	internal diameter of the heating tubes (m)
f	Darcy friction factor
g	acceleration due to gravity (m/s ²)
h_{fg}	latent heat of evaporation (J/kg)
\dot{m}_e	total average evaporation mass flow rate (kg/s)
\dot{m}_{evap}	modelled evaporation mass flow rate (kg/s)
\dot{m}_{in}	juice mass flow rate at vessel inlet (kg/s)
P	pressure (Pa)
Q_{tot}	total thermal energy into the system (W)
Re	Reynolds number
S_c	source term in continuity equation (kg/m ³ /s)
S_m	source term in momentum equation (kg/m ² /s ²)
S_e	source term in energy equation (J/m ³ /s)
T	temperature of the fluid (°C)
T_{bpe}	boiling point elevation temperature (°C)
T_{sat}	saturation temperature (°C)

t	time (s)
u	velocity component in the x direction (m/s)
v	velocity component in the y direction (m/s)
w	velocity component in the z direction (m/s)
X	mass ratio of vapour phase to liquid phase present in any specified volume (fluid quality)
κ	thermal conductivity (W/m/K)
μ	dynamic viscosity (Pa.s)
ρ	density (kg/m ³)

Subscripts

l	denotes the liquid phase
g	denotes the gaseous (vapour) phase
m	denotes average properties of liquid and vapour phase combined
ref	denotes a reference property